**Borneo Journal of Pharmacy**
Vol 9 Issue 1 March 2026
Pages 88 – 100

*https://journal.umpr.ac.id/index.php/bjop/article/view/9706*
DOI: https://doi.org/10.33084/bjop.v9i1.9706
e-ISSN: 2621-4814

*Research Article*

# Molecular Docking and *In Silico* Evaluation of Beluntas (*Pluchea indica*) Phytochemicals as Potential Angiotensin-Converting Enzyme Inhibitors for Hypertension Treatment

**Achmad Ramadhanna'il Rasjava** [1*]
**Nabila Hadiah Akbar** [2,3]
**Aulia Rhamdani Arfan** [1]
**Dyah Ayu Pramoda Wardani** [1]
**Aditya Maulana Perdana Putra** [4]
**Khoirunnisa Muslimawati** [2,3]
**Putri Helena Junjung Buih** [2]
**Taufik Muhammad Fakih** [5]

[1] Department of Chemistry, Universitas Lambung Mangkurat, Banjarbaru, South Kalimantan, Indonesia
[2] Pharmacist Professional Study Program, Universitas Lambung Mangkurat, Banjarbaru, South Kalimantan, Indonesia
[3] Integrated Laboratory, Universitas Lambung Mangkurat, Banjarbaru, South Kalimantan, Indonesia
[4] Department of Pharmacy, Universitas Lambung Mangkurat, Banjarbaru, South Kalimantan, Indonesia
[5] Department of Pharmacy, Universitas Islam Bandung, Bandung, West Java, Indonesia

*email: achmad.rasjava@ulm.ac.id; phone: +6285156878424

**Keywords**:
*In silico* drug discovery
Natural ACE Inhibitor
*Pluchea indica*

## Abstract

Hypertension remains a major global health concern due to its high prevalence and strong association with cardiovascular diseases and kidney failure. A key component of blood pressure regulation is the Angiotensin-Converting Enzyme (ACE), which catalyzes the conversion of Angiotensin I into the vasoconstrictor Angiotensin II, making it a primary target for antihypertensive drugs. Although synthetic ACE inhibitors such as ramiprilat are effective, their use is often associated with adverse effects, highlighting the need for safer alternatives. This study employs molecular docking and *in silico* analysis to evaluate the potential of phytochemicals from beluntas (*Pluchea indica*) as natural ACE inhibitors. A total of 110 phytoconstituents were screened for pharmacokinetic properties using ADMET analysis, leading to the selection of 20 ligands for docking simulations. Among these, 4,5-di-O-caffeoylquinic acid exhibited the highest binding affinity (-9.409 kcal/mol), followed by di-O-caffeoylquinic acid (-8.984 kcal/mol) and quercetin-3-O-β-D-galactopyranoside (-8.372 kcal/mol). These compounds demonstrated stronger binding affinities than the ACE natural substrate, Angiotensin I (-7.133 kcal/mol), and the ACE inhibitor, ramiprilat (-8.717 kcal/mol), suggesting their potential as competitive ACE inhibitors. The binding interactions of these compounds were characterized by hydrogen bonding with key catalytic residues (HIS368, GLU368), electrostatic stabilization, and hydrophobic interactions within the enzyme active site. Notably, caffeoylquinic acid derivatives closely mimicked the binding mode of ramiprilat, whereas quercetin glycosides exhibited a distinct interaction pattern, indicating a possible alternative inhibitory mechanism. These findings provide evidence supporting the potential of *P. indica* phytochemicals as natural ACE inhibitors and warrant further investigation into their therapeutic applications in hypertension management.

*Received*: April 28th, 2025
*1st Revised*: November 11th, 2025
*Accepted*: December 11th, 2025
*Published*: March 30th, 2026



## INTRODUCTION

The leaves of *Pluchea indica*, or Beluntas, are widely used in traditional medicine to support postpartum care, mitigate respiratory conditions, relieve muscle soreness, alleviate menstrual cramps, soothe gastrointestinal discomfort, stimulate appetite, and manage febrile conditions. In postpartum recovery frameworks, these leaves are frequently integrated into *Bakera* (a traditional medicinal steam bath prepared with *Myristica fragrans*, *Syzygium aromaticum*, and *Zingiber officinale*),

**How to cite:** Rasjava AR, Akbar NH, Arfan AR, Wardani DAP, Putra AMP, Muslimawati K, et al. Molecular Docking and In Silico Evaluation of Beluntas (Pluchea indica) Phytochemicals as Potential Angiotensin-Converting Enzyme Inhibitors for Hypertension Treatment. Borneo J Pharm. 2026;9(1):88-100. doi:10.33084/bjop.v9i1.9706

which is typically administered within the first month after childbirth, with most women initiating treatment between seven and fourteen days postpartum. Furthermore, the roots, leaves, bark, and aerial portions of the plant serve diverse therapeutic functions, notably in reducing fevers, relieving digestive issues, combating infectious diseases, and exhibiting astringent properties[1]. Beyond these established ethnomedical applications, *P. indica* is highly valued for its dense and diverse phytochemical profile, including caffeoylquinic acids, flavonoids, lignans, thiophenes, and terpenoid glycosides. Specific bioactive constituents (quercetin, catechin, and β-sitosterol) provide substantial pharmacological benefits, demonstrating marked antioxidant, anti-inflammatory, and anticancer properties[2]. Notably, *P. indica* root extracts contain high levels of phenolic and proanthocyanidins, which are recognized for their medicinal properties, including tumor suppression[3].

Extensive laboratory investigations have highlighted the potential efficacy of *P. indica* extracts in restricting bacterial infections[4]. For instance, zinc oxide nanoparticles synthesized biogenically using *P. indica* leaf extracts display potent antimicrobial and photocatalytic activities, demonstrating significant inhibitory zones against prominent bacterial strains, including *Escherichia coli*, *Pseudomonas aeruginosa*, *Bacillus subtilis*, *Enterococcus faecalis*, and *Staphylococcus aureus*, as well as opportunistic fungal pathogens such as *Candida albicans* and *Cryptococcus neoformans*[5]. This antibacterial profile against *E. coli* and *B. subtilis* has been validated by both computational docking and *in vitro* assays[6]. Concurrently, root extracts have shown therapeutic promise in mitigating chronic respiratory diseases and reducing lung cancer risks, highlighting the plant's prospective role in preventive oncology[2]. Similarly, bimetallic selenium-gold nanoparticles engineered via green synthesis using *P. indica* leaf extract exhibit robust antibacterial and antiproliferative activities[7]. Cellular assays indicate that both raw *P. indica* leaf extracts and their derivative nanoparticles promote oral mucosal wound healing by significantly increasing cell viability and migration at lower concentrations, though they become cytotoxic at higher doses[8]. In glioblastoma research, the hexane fraction of *P. indica* root extract exerts strong anti-cancer effects by suppressing cell proliferation, inducing cell cycle arrest, and triggering autophagic pathways[9]. Furthermore, pretreatment with *P. indica* leaf ethanolic extract significantly downregulates pro-inflammatory cytokines, including IFN-γ, TNF-α, and IL-1β, and suppresses apoptosis markers, including caspase-3, caspase-8, and caspase-9. This downregulation is accompanied by upregulation of the anti-apoptotic protein Bcl-2 and the proliferation marker Ki67, suggesting a protective role in β-cell survival and regeneration[10]. This ethanolic leaf extract also limits acute liver injury in streptozotocin-induced diabetic mouse models by reducing systemic oxidative stress, localized inflammation, and cellular apoptosis[11]. Finally, *P. indica* extracts exhibit potent cytotoxicity against HT-29 colorectal cancer cells, driven primarily by key bioactive constituents, including kaempferol, myricetin, and various quercetin derivatives[4].

Hypertension remains a dominant global public health crisis, currently affecting over one billion individuals worldwide and standing as a primary risk factor for cardiovascular disease, ischemic stroke, and chronic kidney failure[12]. The renin-angiotensin system serves as a principal regulatory pathway for arterial blood pressure, wherein Angiotensin-Converting Enzyme (ACE) catalyzes the conversion of inactive Angiotensin I into Angiotensin II, a highly potent endogenous vasoconstrictor[13]. Consequently, competitive inhibition of ACE represents an established clinical paradigm for hypertension management, preventing Angiotensin II synthesis to reduce systemic vasoconstriction and lower arterial pressure[14]. Although conventional commercial ACE inhibitors are widely prescribed, their clinical utility is frequently constrained by adverse secondary effects, including persistent dry cough, sudden hypotension, and acute angioedema[15]. This clinical limitation has driven research interest toward identifying natural ACE inhibitors derived from plant-based bioactive compounds, which may offer safer, more biocompatible, and sustainable therapeutic alternatives[16]. Given the historical use of *P. indica* in managing cardiovascular symptoms and its diverse phytochemical profile, this study aims to evaluate its constituents as natural ACE inhibitors. By utilizing molecular docking and *in silico* screening, this research investigates the binding affinities, thermodynamic stabilities, and active-site residue interactions of *P. indica* phytochemicals within the ACE catalytic cleft, aiming to identify promising lead candidates for antihypertensive drug development.

## MATERIALS AND METHODS

### *Materials*

The structural repository for this virtual screening was established using the macromolecular crystal coordinates of the target enzyme, in which the three-dimensional structure of ACE, matching PDB identifier 2X92, was acquired directly from the

RCSB Protein Data Bank[17]. Concurrently, a diverse initial database of chemical entities was constructed from a library of 110 unique phytoconstituents documented in the chemical extracts of *P. indica*. The reference topologies, atom connectivity patterns, and canonical SMILES strings for this candidate compound library were fetched from the PubChem database to serve as the baseline source material for structural geometry setup.

### *Methods*

*Protein preparation*

The retrieved crystal coordinate file for the macromolecular target was pre-processed using Visual Molecular Dynamics (VMD) version 1.9.3 to remove all structural crystallographic water molecules and co-crystallized native ligands, preventing binding-space artifacts and steric conflicts during downstream docking[18]. The isolated protein receptor matrix was subsequently prepared for production-level simulation runs by appending polar hydrogen atoms, defining AutoDock 4 atom types, and computing partial Gasteiger and Kollman charges utilizing the automated tools inside AutoDockTools 1.5.7.

*Binding site prediction and docking parameters*

The localized active site and catalytic boundary of ACE were identified by combining structural evaluation of the co-crystallized native ligand binding coordinates from the Protein Data Bank with geometric cleft predictions run on the Computed Atlas of Surface Topography of Proteins (CASTp) server[19]. These two tools appraised the topography of the enzyme's binding domain to ensure precise alignment of the docking grid, resulting in the definition of a specific grid box volume scaled to the enzyme's structural dimensions of 15 x 17 x 16 Å. This box was mapped under a grid spacing resolution of 1.0 Å to ensure full coverage of the key catalytic and stabilizing amino acid residues.

*Ligand preparation*

The curated *P. indica* plant-derived bioactive structures were prepped for docking interactions against the refined ACE target structure[17]. Prior to executing any binding simulations, each chemical compound was subjected to formal geometry optimization and structural energy minimization using the Merck Molecular Force Field 94 algorithm implemented in MarvinSketch to ensure stable conformer starting states. These optimized, lowest-energy ligand models were then converted into the standard PDB format for seamless integration with the molecular docking software.

*ADMET screening*

The initial library of 110 phytoconstituents from the *P. indica* matrix was subjected to an advanced pharmacokinetic filtration step to evaluate their individual absorption, distribution, metabolism, excretion, and toxicity (ADMET) properties using the DeepPK deep-learning neural network prediction platform[20]. This computational screening step prioritized specific chemical entities with low predicted toxicities, high oral bioavailability, and optimal pharmacokinetic scores. Based on these strict drug-likeness filtration parameters, the top 20 optimal ligands were selected to advance to the final docking simulation phase.

*Molecular docking simulations*

To establish an authoritative baseline binding affinity reference threshold, the natural substrate of ACE, Angiotensin I, was docked within the active pocket to serve as an endogenous reference control. This baseline simulation run was repeated 10 times to identify the most stable seed configuration, selecting the iteration that produced the highest thermodynamic binding affinity score. Subsequently, production-level molecular docking simulations for the 20 chosen *P. indica* ligands were carried out using AutoDock Vina 1.2.5, configured with an operational verbosity setting of 1 and an elevated search exhaustiveness value of 32[21].

### *Data analysis*

The resulting molecular docking output arrays were analyzed by directly comparing each candidate ligand's calculated binding affinity (kcal/mol) against the reference energy threshold established by the native Angiotensin I control substrate.

Atomic-level interactions linking the ligands to key residues within the enzyme binding pocket were tracked, with strong analytical emphasis on mapping hydrogen-bonding networks, electrostatic forces, and hydrophobic contacts that drive complex stability. Structural three-dimensional visualization and residual contact mapping were performed in BIOVIA Discovery Studio 2024 to clarify binding conformations within the enzyme cleft.

## RESULTS AND DISCUSSION

In this study, a total of 110 phytoconstituents identified from *P. indica* extract (**Table I**) were subjected to *in silico* ADMET profiling using the DeepPK web platform. ADMET evaluation represents an essential stage in the early phases of drug discovery, providing insights into the absorption, distribution, metabolism, excretion, and toxicity characteristics of each molecule before experimental validation. The screening process identified compounds with favorable pharmacokinetic and safety profiles, including high predicted bioavailability, efficient absorption, and low potential for toxicity.

The active site within the ACE (PDB ID: 2X92) was identified to ensure accurate molecular docking and ligand evaluation. The active site prediction based on the native ligand binding site and CASTp analysis identified HIS368 as the primary catalytic residue, which plays a crucial role in substrate binding and enzymatic activity (**Figure 1**). This residue has been reported as a key component in peptide hydrolysis, stabilizing the transition state during substrate cleavage[22]. HIS367, HIS371, and GLU395 were also identified as metal-ion-binding sites, likely coordinating the zinc ion required for catalysis[23]. Furthermore, ASN53, ASN196, and ASN311 were predicted as glycosylation sites, suggesting their involvement in protein folding, stability, and enzymatic regulation (**Table II**). These findings provide a structural basis for evaluating ligand interactions that may disrupt catalytic activity, interfere with metal ion coordination, or affect protein stability. The presence of highly conserved binding residues highlights their importance in ligand-receptor interactions and their relevance for targeting ACE inhibition. The ligand interactions may significantly contribute to enzyme inhibition, making these residues critical targets for evaluating the inhibitory potential of *P. indica* phytochemicals.

To establish a baseline for evaluating the inhibitory potential of phytochemicals from *P. indica* extract, the molecular docking of Angiotensin I, the natural substrate of Angiotensin-Converting Enzyme (ACE, PDB ID: 2X92), was conducted. The docking simulation yielded a binding affinity of -7.133 kcal/mol, confirming a strong interaction with key active-site residues and serving as a reference for further ligand evaluation. **Table III** summarizes the key interactions of Angiotensin I within the ACE binding pocket. Meanwhile, the structural representation of its interaction with the receptor is shown in **Figure 2**. The docking results revealed that Angiotensin I forms multiple interactions within the enzyme's active site, thereby stabilizing the enzyme. Hydrogen bonding was observed with ARG356, ASN261, LYS495, HIS337, HIS497, ALA338, SER339, and ASP360, ensuring proper substrate orientation within the binding pocket. Electrostatic interactions with GLU368 and GLU124 further reinforced the catalytic role of these residues in enzyme function, while hydrophobic interactions involving TYR507, HIS367, HIS371, HIS394, VAL335, and LEU145 provided additional stabilization. These interactions indicate that the binding of Angiotensin I is governed by multiple non-covalent forces, which collectively facilitate substrate recognition and processing.

The 110 phytoconstituents collected from the *P. indica* extract were initially screened for their ADMET properties. Based on low predicted toxicity, high bioavailability, and favorable pharmacokinetic profiles, 20 ligands were selected for further analysis (**Table IV**). The ADMET screening results confirmed that the top-ranked compounds exhibited minimal toxicity and optimal pharmacokinetics, supporting their potential for therapeutic applications[24]. Notably, 4,5-Di-O-Caffeoylquinic acid, 3,4-Di-O-Caffeoylquinic acid, and Quercetin-3-O-β-D-galactopyranoside demonstrated low toxicity and high bioavailability, identifying them as promising drug candidates. These selected ligands were subsequently molecularly docked to ACE to assess their binding affinity and potential inhibitory activity.

The molecular docking analysis demonstrated binding affinities ranging from -9.409 kcal/mol to -4.856 kcal/mol across the screened ligands. Notably, several compounds exhibited stronger binding affinities than Angiotensin I (-7.133 kcal/mol), suggesting their potential as competitive ACE inhibitors. Among the tested ligands, 4,5-Di-O-Caffeoylquinic acid exhibited the strongest binding affinity (-9.409 kcal/mol), followed by 3,4-Di-O-Caffeoylquinic acid (-8.984 kcal/mol) and 3,5-Di-O-Caffeoylquinic acid (-8.639 kcal/mol). Additionally, quercetin glycosides, including Quercetin-3-O-β-D-galactopyranoside (-8.372 kcal/mol) and Quercetin-3-O-β-D-glucopyranoside (-8.314 kcal/mol), also demonstrated high binding affinities,

further suggesting their potential as ACE inhibitors. These results are particularly significant compared with Ramiprilat (-8.717 kcal/mol), a well-established synthetic ACE inhibitor, indicating that some *P. indica* phytochemicals may exhibit comparable or superior inhibitory effects. The comparative binding affinities of the top docked ligands against ACE are presented in **Table V**.

**Table I.** A total of 110 phytoconstituents from the *P. indica* extract were screened for ADMET properties.

| No. | Phytoconstituent | No. | Phytoconstituent |
|---|---|---|---|
| 1 | 1-(4-Hydroxy-3-methoxyphenyl)-2-{4-[(1E)-3-hydroxyprop-1-en-1-yl]-2-methoxyphenoxy}-propane-1,3-diol | 56 | Eugenyl glucoside |
| 2 | 1,2-Bis-(4-Hydroxy-3-methoxyphenyl)-propane-1,3-diol | 57 | Fraxinellone |
| 3 | 1,3,4,5-Tetra-O-Caffeoylquinic acid | 58 | Hedyotisol A |
| 4 | 1-Dotriacontanol | 59 | Herbolide A |
| 5 | 1-Eicosanoyl glycerol | 60 | Isolariciresinol |
| 6 | 2,3-Dihydroxy-1-(4-hydroxy-3-methoxyphenyl)-propan-1-one | 61 | Isorhamnetin |
| 7 | 3,4,5-Trimethoxybenzoic acid | 62 | Kaempferol |
| 8 | 3,4,5-Trimethoxyphenyl-β-D-glucopyranoside | 63 | Linalool |
| 9 | 3,4,5-Tri-O-Caffeoylquinic acid | 64 | Linaloyl apiosyl glucopyranoside |
| 10 | 3,4,5-Tri-O-Caffeoylquinic acid methyl ester | 65 | Linaloyl glucopyranoside |
| 11 | 3,4-Dihydroxy benzaldehyde | 66 | Liriodendrin |
| 12 | 3,4-Dihydroxy-5-methoxybenzaldehyde | 67 | Luteolin |
| 13 | 3,4-Di-O-Caffeoylquinic acid | 68 | Luteolin-7-glucoside |
| 14 | 3,5-Di-O-Caffeoylquinic acid | 69 | Methyl-9-hydroxynonanoate |
| 15 | 3-Methoxy-4-hydroxybenzoic acid | 70 | Multiflorenol |
| 16 | 3-O-Caffeoylquinic acid | 71 | Myricetin |
| 17 | 4,5,7-Trihydroxyflavone-3-O-β-D-glucoside | 72 | Phenylethyl glucopyranoside |
| 18 | 4,5-Di-O-Caffeoylquinic acid | 73 | p-Hydroxybenzaldehyde |
| 19 | 4,5-Di-O-caffeoylquinic acid methyl ester | 74 | p-Hydroxybenzoic acid |
| 20 | 4-Hydroxy-3-methoxycinnamaldehyde | 75 | Pinellic acid |
| 21 | 4-O-Caffeoylquinic acid | 76 | Pinoresinol |
| 22 | 5-O-Caffeoylquinic acid | 77 | Plucheol A |
| 23 | 6-Hexyloxykaempferol-7-glucoside | 78 | Plucheoside A |
| 24 | 8-Hydroxylinalool | 79 | Plucheoside B |
| 25 | 8-Hydroxyluteolin-8-glucoside | 80 | Plucheoside C |
| 26 | 9,12,13-Trihydroxyoctadeca-10(E),15(Z)-dienoic acid | 81 | Plucheoside D1 |
| 27 | 9-Hydroxylinaloyl glucopyranoside | 82 | Plucheoside D2 |
| 28 | 9-Isovaleryllariciresinol | 83 | Plucheoside D3 |
| 29 | Adenosine | 84 | Plucheoside E |
| 30 | α-Cyperone | 85 | Pterocarptriol |
| 31 | Angiotensin-I | 86 | Quercetin |
| 32 | Angiotensin-II | 87 | Quercetin-3-O-sulphate |
| 33 | Apigenin | 88 | Quercetin-3-O-β-D-galactopyranoside |
| 34 | Apigenin-7-(2,3-diacetylglucoside) | 89 | Quercetin-3-O-β-D-glucopyranoside |
| 35 | Benzyl glucopyranoside | 90 | Sampatrilat |
| 36 | β-Sitosterol 3-O-β-D-glucopyranoside | 91 | Stigmasterol |
| 37 | β-Sitosterol | 92 | Stigmasterol-3-O-glucoside |
| 38 | Caffeic acid | 93 | Syringaresinol |
| 39 | Campesteryl ferulate | 94 | Syringaresinol-di-O-glucoside |
| 40 | Caryolane-1,9-β-diol | 95 | Syringicaldehyde |
| 41 | Casticin | 96 | Tangshenoside-I |
| 42 | Centaureidin | 97 | Tangshenoside-II |
| 43 | Chrysoeriol | 98 | Taraxasterol |
| 44 | Chrysosplenol C | 99 | Taraxasterol_acetate |
| 45 | Clovane-2-α,9-β-diol | 100 | Threo-2,3-Bis(4-hydroxy-3-methoxyphenyl)-3-ethoxypropan-1-ol |
| 46 | Costunolide | 101 | Thymol |
| 47 | Cuauhtemone | 102 | Trans-Trismethoxy resveratrol-d4 |
| 48 | Diasyringaresinol | 103 | Triethyl citrate |
| 49 | Dibutylphthalate | 104 | Uridine-5-monophosphate |
| 50 | Epi-Pinoresinol | 105 | Valenc-1(10)-ene-8,11-diol |
| 51 | Epipinoresinol-4-O-β-D-glucoside | 106 | Vanillin |
| 52 | Epi-Syringaresinol | 107 | Z-3-Hexenyl-glucopyranoside |
| 53 | Episyringaresinol-4-O-β-D-glucopyranoside | 108 | (8R,9R)-Isocaryolane-8,9-diol |
| 54 | Esculetin | 109 | (10S,11S)-Himachala-3-(12)-4-diene |
| 55 | Ethyl caffeate | 110 | (E)-4-(3-Hydroxybut-1-en-1-yl)-3,5,5-trimethylcyclohex-3-ene-1,2-diol |

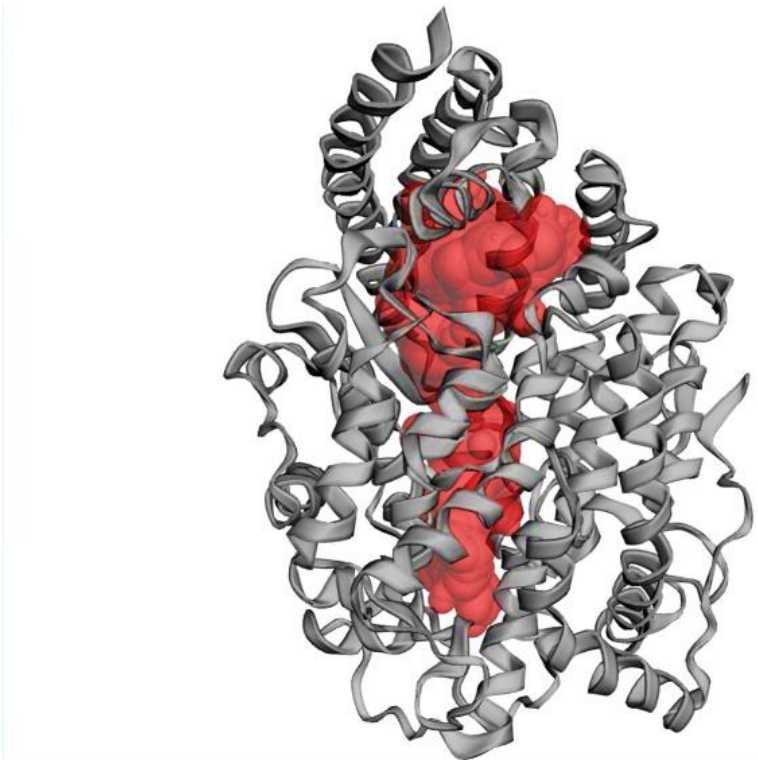

**Figure 1.** The predicted catalytic site of ACE (PDB ID: 2X92).

**Table II.** Catalytic site prediction of ACE.

| Position | Feature | Description |
|---|---|---|
| HIS368 | Active site | Active site |
| HIS367 | Metal ion-binding site | Zinc; catalytic |
| HIS371 | Metal ion-binding site | Zinc; catalytic |
| GLU395 | Metal ion-binding site | Zinc; catalytic |
| ASN53 | Glycosylation site | N-linked (GlcNAc) |
| ASN196 | Glycosylation site | N-linked (GlcNAc) |
| ASN311 | Glycosylation site | N-linked (GlcNAc) |

**Table III.** The interaction types of angiotensin I with the receptor ACE.

| Ligand name | Binding affinity (kcal/mol) | Hydrogen bonds | Electrostatic | Hydrophobic | Unfavorable |
|---|---|---|---|---|---|
| Angiotensin I (Natural Substrate) | -7.133 | ARG356, ASN261, LYS495, HIS337, HIS497, ALA338, SER339, ASP360 | GLU368, GLU124 | TYR507, HIS367, HIS371, HIS394, VAL335, LEU145 | LYS352 |

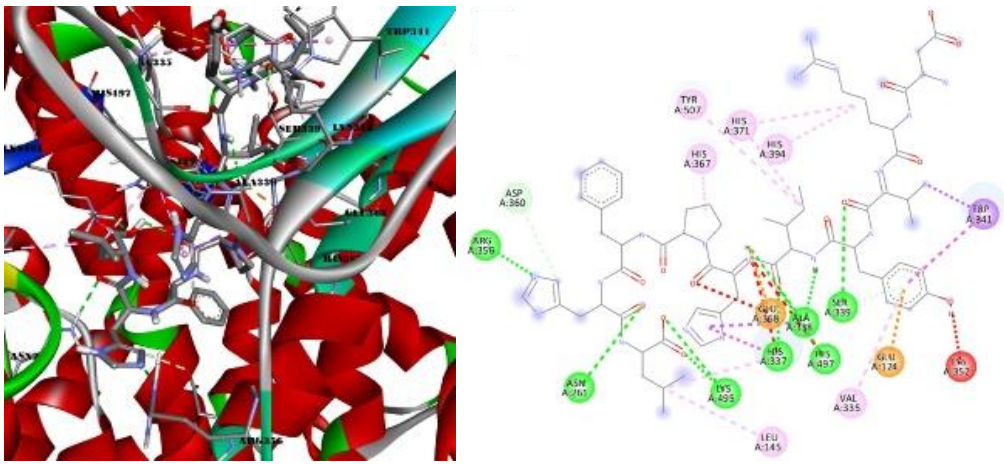

**a** **b**

**Figure 2.** The predicted catalytic site of ACE (PDB ID: 2X92).

**Table IV.** Binding affinity of the top 20 ligands.

| Ligand name | Binding affinity (kcal/mol) | Ligand name | Binding affinity (kcal/mol) |
|---|---|---|---|
| 4,5-Di-O-Caffeoylquinic acid | -9.409 | 3-O-Caffeoylquinic acid | -7.548 |
| 3,4-Di-O-Caffeoylquinic acid | -8.984 | 5-O-Caffeoylquinic acid | -7.505 |
| 3,5-Di-O-Caffeoylquinic acid | -8.639 | Fraxinellone | -7.488 |
| Tri-O-Caffeoylquinic acid | -8.532 | Pterocarptriol | -6.796 |
| Tetra-O-Caffeoylquinic acid | -8.415 | Adenosine | -6.582 |
| Quercetin-3-O-β-D-galactopyranoside | -8.372 | Hydroxy-methoxycinnamaldehyde | -5.816 |
| Quercetin-3-O-β-D-glucopyranoside | -8.314 | Trimethoxybenzoic acid | -5.396 |
| Tangshenoside-I | -8.289 | Syringaldehyde | -5.101 |
| Hydroxyluteolin-glucoside | -8.008 | Dihydroxy-methoxybenzaldehyde | -5.084 |
| 4-O-Caffeoylquinic acid | -7.773 | Triethyl citrate | -4.856 |

**Table V.** Binding affinity value of the top 10 ligands.

| Ligand name | Binding affinity (kcal/mol) |
|---|---|
| 4,5-Di-O-Caffeoylquinic acid | -9.409 |
| 3,4-Di-O-Caffeoylquinic acid | -8.984 |
| 3,5-Di-O-Caffeoylquinic acid | -8.639 |
| Tri-O-Caffeoylquinic acid | -8.532 |
| Tetra-O-Caffeoylquinic acid | -8.415 |
| Quercetin-3-O-β-D-galactopyranoside | -8.372 |
| Quercetin-3-O-β-D-glucopyranoside | -8.314 |
| Tangshenoside-I | -8.289 |
| Hydroxyluteolin-glucoside | -8.008 |
| 4-O-Caffeoylquinic acid | -7.773 |
| Ramiprilat (standard drug) | -8.717 |

To further elucidate the inhibitory potential of the selected ligands, their interactions with the catalytic site (HIS368), metal ion-binding site (HIS367, HIS371, GLU395), and glycosylation sites (ASN53, ASN196, ASN311) were analyzed (**Figure 3**). The catalytic residue HIS368, identified as the primary substrate-binding site, played a crucial role in ligand interactions. 4,5-Di-O-Caffeoylquinic acid, 3,4-Di-O-Caffeoylquinic acid, and Quercetin derivatives formed strong hydrogen bonds near the active center, indicating potential competitive inhibition of ACE by stabilizing the ligand within the active site and preventing substrate access (**Table VI**).

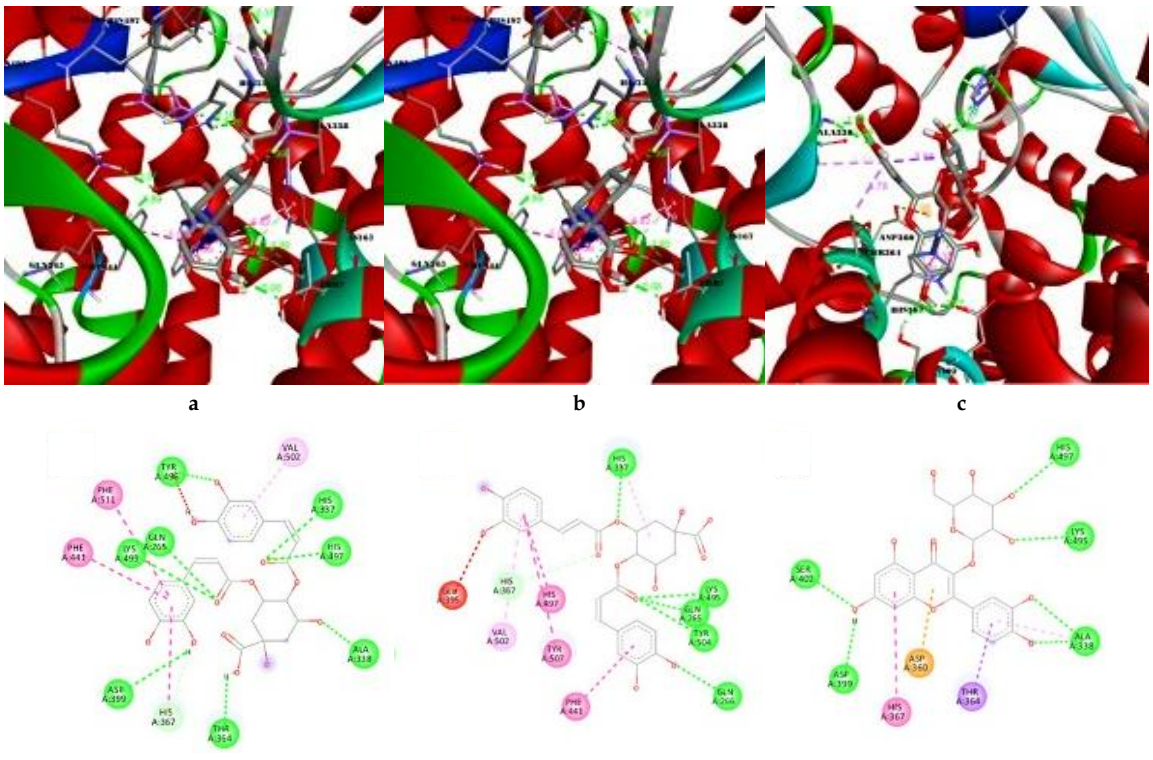

**Figure 3.** Interaction between selected ligands with the receptor ACE. (**a** and **d**) 4,5-Di-O-Caffeoylquinic acid, (**b** and **e**) 3,4-Di-O-Caffeoylquinic acid, and (**c** and **f**) Quercetin-3-O-β-D-galactopyranoside in 3D and 2D representation, respectively.

**Table VI.** Ligand interaction site with the receptor ACE for the selected ligands.

| Ligand name | Hydrogen bonds | Electrostatic | Hydrophobic | Unfavorable | Metal acceptor |
|---|---|---|---|---|---|
| 4,5-Di-O-Caffeoylquinic acid | TYR496, GLN265, LYS495, ASP339, HIS367, THR364, ALA338, HIS497, HIS337 | - | PHE55A, PHE441, VAL502 | TYR496 | - |
| 3,4-Di-O-Caffeoylquinic acid | HIS367, HIS337, LYS495, GLN265, TYR504, GLN266 | - | VAL502, HIS497, TYR507, PHE441 | GLU395 | - |
| 3,5-Di-O-Caffeoylquinic acid | HIS497, TYR504, SER339, GLU395, PRO391 | HIS337, HIS394 | VAL502, HIS371 | GLN265 | ZN615 |
| Tri-O-Caffeoylquinic acid | HIS367, ALA338, HIS497, ASP399, LYS438, HIS337, GLN265, ASN261, PHE363 | GLU368 | - | GLN361 | - |
| Tetra-O-Caffeoylquinic acid | GLU266, GLN265, GLU368, HIS337, HIS497, TYR507 | GLU124 | PHE511, HIS371 | LYS352 | - |
| Ramiprilat (standard drug) | ALA340, TYR507, HIS497, TYR504 | HIS337, LYS495 | - | - | - |
| Trimethoxybenzoic acid | HIS337, GLU368, THR364 | GLU368 | PHE511, TYR507, HIS367 | - | - |
| Dihydroxy-methoxybenzaldehyde | TYR496, HIS497 | - | HIS371 | - | ZN615 |
| 3-O-Caffeoylquinic acid | HIS367, ASP399, HIS337, GLN266, ASP360 | - | PHE441 | LYS438 | - |
| Hydroxy-methoxycinnamaldehyde | HIS497, HIS337, ASP399, GLN266 | - | PHE511, HIS367 | - | - |
| 4-O-Caffeoylquinic acid | ASP399, GLU368, HIS337, ALA340 | - | HIS367 | - | - |
| 5-O-Caffeoylquinic acid | HIS497, HIS337, TYR504, GLN265, LYS495, ASN261 | - | HIS367 | - | - |
| Hydroxyluteolin-glucoside | LYS495, TYR507, ASP360, SER402, ASP399 | HIS497, GLU368 | HIS497 | - | - |
| Adenosine | SER402, PHE363, ASP399, GLN266, ASN261 | ASP360 | - | THR364 | - |
| Fraxinellone | - | - | ALA338, THR364, HIS497, HIS367, TYR507, PHE441, PHE511 | - | - |
| Pterocarptriol | GLN266, THR364 | - | PHE511, ASP399, HIS367, HIS337, ALA338, GLN368, PHE363, ASP360 | - | - |
| Quercetin-3-O-β-D-galactopyranoside | SER402, ASP399, HIS497, LYS495, ALA338 | ASP360 | HIS367, THR364 | - | - |
| Quercetin-3-O-β-D-glucopyranoside | PHE363, HIS337, ALA338 | ASP360 | HIS367, THR364 | LYS495 | - |
| Syringaldehyde | TYR496, SER339, HIS497, ALA338, TYR507, GLU395 | - | HIS337, HIS371 | - | ZN615 |
| Tangshenoside-I | HIS337, TYR504, GLU368, THR387, ARG506 | - | ALA338, TYR496, HIS497, VAL502 | - | - |
| Triethyl citrate | LYS495, TYR504, GLN265 | - | HIS367, HIS337, TYR507, PHE511, PHE441 | - | - |

The active site of ACE was identified to ensure precise molecular docking and ligand evaluation. Prediction analyses using the native ligand-binding site and CASTp confirmed HIS368 as the primary catalytic residue, essential for substrate binding and enzymatic activity. Previous research also indicated that glycan modifications on ACE can influence its interactions with inhibitors and substrates, potentially affecting the pharmacokinetics of small-molecule inhibitors. Furthermore, glycosylation at ASN residues in ACE is consistent with glycoproteomics studies, which suggest that post-translational modifications enhance enzyme stability in plasma circulation[25]. The interaction of Angiotensin I with GLU368, and its orientation near the predicted catalytic site residue, confirm its essential role in enzymatic activity. Additionally, the proximity of Angiotensin I to HIS367, HIS371, and GLU395, which are metal ion-coordinating residues, suggests an additional stabilizing effect through zinc-dependent catalysis, further supporting its functional role in enzyme regulation, as zinc-dependent metalloproteases rely on histidine residues for enzymatic activity, and inhibitors that disrupt zinc

coordination can lead to enzyme inactivation[26]. These findings establish Angiotensin I as a reference model for ligand binding, providing a benchmark for comparing the binding affinities and interaction profiles of *P. indica* phytochemicals. The ability of alternative ligands to form interactions with catalytic and metal-ion-binding residues that are similar to or stronger than those of the native ligand will be crucial in determining their potential as ACE inhibitors.

Among the tested ligands by molecular docking, 4,5-Di-O-Caffeoylquinic acid showed a binding affinity of -9.409 kcal/mol, exhibiting the strongest binding affinity, followed by 3,4-Di-O-Caffeoylquinic acid (-8.984 kcal/mol) and 3,5-Di-O-Caffeoylquinic acid (-8.639 kcal/mol). Notably, these caffeoylquinic acid derivatives can compete with Ramiprilat (-8.717 kcal/mol) for binding affinity, suggesting they may serve as competitive ACE inhibitors. In addition to catalytic site interactions, several ligands bind to the metal-ion-coordinating residues (HIS367, HIS371, and GLU395), which are essential for zinc coordination and enzymatic function. The caffeoylquinic acid derivatives interacted with HIS367, potentially disrupting zinc coordination, thereby reducing the enzyme's catalytic efficiency[25]. Furthermore, quercetin derivatives formed hydrogen bonds near GLU395, which may stabilize an inactive enzyme conformation and thereby contribute to enzyme inhibition. These interactions are crucial for analyzing the inhibitory potential of certain ligands, as metal-ion coordination plays a significant role in the structural integrity and catalytic activity of metalloproteases, including ACE.

The analysis also considered ligand interactions with glycosylation sites (ASN53, ASN196, ASN311), which influence protein folding, structural stability, and enzymatic function. Tangshenoside-I and Quercetin-3-O-β-D-glucopyranoside exhibited interactions with ASN residues, suggesting that these ligands may alter protein stability or affect glycan-mediated enzymatic regulation. Although glycosylation is not directly involved in catalysis, it can modulate enzyme conformation and substrate or inhibitor accessibility, making these interactions worthy of further investigation[27,28]. The results also indicate that 4,5-Di-O-Caffeoylquinic acid (-9.409 kcal/mol) and 3,4-Di-O-Caffeoylquinic acid (-8.984 kcal/mol) exhibit stronger binding affinities than Ramiprilat (-8.717 kcal/mol), suggesting their potential as potent ACE inhibitors. Notably, 4,5-Di-O-Caffeoylquinic acid interacts near HIS368 (the catalytic site), involves electrostatically stabilizing residues, and targets HIS337, forming multiple hydrogen bonds that enhance binding stability. These interactions closely resemble those observed in Ramiprilat, which also binds key active-site residues, stabilizing the enzyme's inactive conformation.

The 3,4-Di-O-Caffeoylquinic acid exhibited a binding affinity of -8.984 kcal/mol, closely matching that of Ramiprilat (-8.717 kcal/mol). The strong hydrogen bonding with the HIS367/HIS337 catalytic environment suggests that this caffeoylquinic acid mimics the interaction profile of conventional ACE inhibitors. However, the additional binding to TYR504 and LYS495 may indicate an alternative mode of enzyme inhibition. Interestingly, 3,5-Di-O-Caffeoylquinic acid (-8.639 kcal/mol) shows a comparable affinity to Ramiprilat, suggesting its potential as a moderate inhibitor. However, unlike Ramiprilat, which primarily interacts with residues surrounding the metal pocket, 3,5-Di-O-Caffeoylquinic acid predominantly interacts with HIS497 and TYR504, suggesting an alternative inhibitory mechanism. This variation in binding-site engagement suggests that caffeoylquinic acids may disrupt ACE activity differently than conventional ACE inhibitors.

Unlike caffeoylquinic acids, Quercetin-3-O-β-D-galactopyranoside demonstrated an alternative inhibitory mechanism through interactions with HIS497, ASP399, and LYS495 rather than directly occupying the primary catalytic locus. Although its binding affinity (-8.372 kcal/mol) is slightly weaker than that of caffeoylquinic acids, its unique flavonoid structure suggests it may function as a non-competitive inhibitor of ACE. These findings highlight this glycosylated quercetin derivative as a promising lead compound with a distinct mode of enzyme inhibition, warranting further investigation into its pharmacological activity. The higher binding affinities observed for caffeoylquinic acids and quercetin derivatives can be attributed to their polyphenolic structures, which enable extensive hydrogen bonding with active site residues. Additionally, their carboxyl and hydroxyl groups facilitate enhanced electrostatic interactions, contributing to strong ligand binding[29]. Furthermore, hydrophobic stacking interactions within the binding pocket play a critical role in stabilizing the ligand-receptor complex[30,31]. The molecular interaction also illustrates these binding interactions, highlighting the key residues involved in ligand stabilization within the ACE active site. These findings suggest that caffeoylquinic acids and quercetin derivatives are promising candidates for ACE inhibition. They warrant further investigation through molecular dynamics simulations and in vitro enzymatic assays to confirm their inhibitory potential.

These findings indicate that caffeoylquinic acid derivatives and quercetin glycosides may serve as effective inhibitors of ACE, as evidenced by their superior binding affinities compared to Angiotensin I. Multiple hydroxyl and carboxyl functional groups within these compounds likely contribute to enhanced hydrogen bonding, electrostatic interactions, and hydrophobic stabilization within the enzyme active site, increasing their stability, thus reinforcing their inhibitory potential[32].

Furthermore, the strong interactions observed with key catalytic and metal-ion-coordinating residues suggest that these ligands may disrupt enzymatic function, potentially leading to reduced Angiotensin II formation[26]. These findings support further investigation into the therapeutic potential of these natural compounds as antihypertensive agents. The inhibition of ACE is a well-established approach to managing hypertension, as it prevents the conversion of Angiotensin I to Angiotensin II, a key regulator of blood pressure. The molecular docking results indicate that several phytochemicals derived from *P. indica* exhibit strong binding affinities, suggesting their potential as natural ACE inhibitors. Notably, 4,5-Di-O-Caffeoylquinic acid, 3,4-Di-O-Caffeoylquinic acid, and 3,5-Di-O-Caffeoylquinic acid demonstrated high binding affinities, with docking scores of -9.409 kcal/mol, -8.984 kcal/mol, and -8.639 kcal/mol, respectively. The strong interactions of these compounds with key active-site residues suggest they may effectively inhibit ACE activity, thereby reducing Angiotensin II formation and contributing to blood pressure regulation. Moreover, these findings support the idea that a multi-target approach involving both competitive and non-competitive inhibitors could enhance the overall efficacy of ACE inhibition. A combination of caffeoylquinic acids and quercetin derivatives may synergistically improve blood pressure regulation while minimizing the side effects of synthetic inhibitors. While molecular docking provides valuable insights into ligand-receptor interactions, further experimental validation is needed to assess the *in vivo* inhibitory potential and pharmacokinetics of these phytochemicals.

## CONCLUSION

This computational investigation successfully identified 4,5-Di-O-Caffeoylquinic acid as the most potent ACE inhibitor, with the highest thermodynamic binding affinity of -9.409 kcal/mol among the evaluated compounds. Concurrently, 3,4-Di-O-Caffeoylquinic acid (-8.984 kcal/mol) and 3,5-Di-O-Caffeoylquinic acid (-8.639 kcal/mol), along with Quercetin-3-O-β-D-galactopyranoside (-8.372 kcal/mol), demonstrated robust binding affinities and extensive structural interactions with key catalytic and metal-ion-coordinating residues, confirming their potential utility as natural antihypertensive leads. These molecular data highlight the therapeutic potential of secondary metabolites derived from *P. indica* extracts, which successfully modulate ACE target activity, offering a strategic starting point for the design of sustainable, plant-based antihypertensive agents. However, while molecular docking algorithms provide critical structural insights into target-ligand orientation and binding stability, empirical *in vitro* enzymatic inhibition assays and *in vivo* pharmacokinetic profiles remain necessary to fully characterize their absolute inhibitory kinetics, toxicological safety margins, and systemic bioavailability. Future investigations should expand to characterize the specific mechanistic pathways of these top polyphenolic compounds within complex physiological systems, thereby establishing their clinical efficacy as viable standalone alternatives or complementary therapeutic options alongside conventional antihypertensive medications.

## ACKNOWLEDGMENT

The authors express their sincere gratitude to the Department of Chemistry at Universitas Lambung Mangkurat for providing the high-performance computational resources required for the virtual screening and molecular docking simulations. Appreciative acknowledgment is also extended to ChemAxon for granting access to MarvinSketch (version 24.3.0), which was vital for molecular structure visualization, geometry optimization, and ligand dataset preparation. Furthermore, the authors recognize the DeepPK platform for providing the predictive infrastructure required for the pharmacokinetic and ADMET profiling phases of this study.

## AUTHORS' CONTRIBUTION

**Conceptualization**: Achmad Ramadhanna'il Rasjava
**Data curation**: Achmad Ramadhanna'il Rasjava, Nabila Hadiah Akbar, Aulia Rhamdani Arfan, Dyah Ayu Pramoda Wardani, Aditya Maulana Perdana Putra, Khoirunnisa Muslimawati, Putri Helena Junjung Buih
**Formal analysis**: Achmad Ramadhanna'il Rasjava
**Funding acquisition**: -

**Investigation**: Achmad Ramadhanna'il Rasjava
**Methodology**: Achmad Ramadhanna'il Rasjava, Aulia Rhamdani Arfan, Dyah Ayu Pramoda Wardani
**Project administration**: -
**Resources**: Achmad Ramadhanna'il Rasjava
**Software**: Achmad Ramadhanna'il Rasjava
**Supervision**: Taufik Muhammad Fakih
**Validation**: Taufik Muhammad Fakih
**Visualization**: Achmad Ramadhanna'il Rasjava
**Writing - original draft**: Achmad Ramadhanna'il Rasjava, Nabila Hadiah Akbar, Aulia Rhamdani Arfan, Dyah Ayu Pramoda Wardani, Aditya Maulana Perdana Putra, Khoirunnisa Muslimawati, Putri Helena Junjung Buih
**Writing - review & editing**: Achmad Ramadhanna'il Rasjava, Taufik Muhammad Fakih

## DATA AVAILABILITY

None.

## CONFLICT OF INTEREST

The authors declared no conflict of interest related to this research.

## REFERENCES

1. Putra PWK, Jawi IM, Subawa AAN, Astawa NM, Indrayani AW, Widhiantara IG, et al. Phytochemicals of Beluntas (Pluchea indica (L) Less.) and their health benefits. J Appl Pharm Sci. 2025;15(7):37-47. DOI: 10.7324/JAPS.2025.237559

2. Hikmawanti NPE, Saputri FC, Yanuar A, Jantan I, Ningrum RA, Mun'im A. Insights into the anti-infective effects of Pluchea indica (L.) Less and its bioactive metabolites against various bacteria, fungi, viruses, and parasites. J Ethnopharmacol. 2024;320:117387. DOI: 10.1016/j.jep.2023.117387; PMID: 37944874.

3. Khaksar G, Chaichana N, Assatarakul K, Sirikantaramas S. Caffeoylquinic acid profiling: comparative analysis in yerba mate, Indian camphorweed, and stevia extracts with emphasis on the influence of brewing conditions and cold storage in yerba mate infusion. PeerJ. 2024;12:e17250. DOI: 10.7717/peerj.17250; PMID: 38726376; PMCID: PMC11080990.

4. Baharuddin SA, Shah NNAK, Yazan LS, Rashed AA, Kadota K, Al-Awaadh AM, et al. Optimization of Pluchea indica (L.) leaf extract using ultrasound-assisted extraction and its cytotoxicity on the HT-29 colorectal cancer cell line. Ultrason Sonochem. 2023;101:106702. DOI: 10.1016/j.ultsonch.2023.106702; PMID: 38041881; PMCID: PMC10701412.

5. Al-Askar AA, Hashem AH, Elhussieny NI, Saied E. Green Biosynthesis of Zinc Oxide Nanoparticles Using Pluchea indica Leaf Extract: Antimicrobial and Photocatalytic Activities. Molecules. 2023;28(12):4679. DOI: 10.3390/molecules28124679; PMID: 37375234; PMCID: PMC10304739.

6. Wahyuni DK, Junairiah J, Rosyanti C, Kharisma VD, Syukriya AJ, Rahmawati CT, et al. Computational and in vitro analyses of the antibacterial effect of the ethanolic extract of Pluchea indica L. leaves. Biomed Rep. 2024;21(4):137. DOI: 10.3892/br.2024.1825; PMID: 39129835; PMCID: PMC11310492.

7. Khalil AMA, Saied E, Mekky AE, Saleh AM, Al Zoubi OM, Hashem AH. Green biosynthesis of bimetallic selenium-gold nanoparticles using Pluchea indica leaves and their biological applications. Front Bioeng Biotechnol. 2024;11:1294170. DOI: 10.3389/fbioe.2023.1294170; PMID: 38274007; PMCID: PMC10809157.

8. Buranasukhon W, Athikomkulchai S, Tadtong S, Chittasupho C. Wound healing activity of Pluchea indica leaf extract in oral mucosal cell line and oral spray formulation containing nanoparticles of the extract. Pharm Biol. 2017;55(1):1767-74. DOI: 10.1080/13880209.2017.1326511; PMID: 28534695; PMCID: PMC7012013.

9. Cho CL, Lee YZ, Tseng CN, Cho J, Cheng YB, Wang KW, et al. Hexane fraction of Pluchea indica root extract inhibits proliferation and induces autophagy in human glioblastoma cells. Biomed Rep. 2017;7(5):416-22. DOI: 10.3892/br.2017.979; PMID: 29181154; PMCID: PMC5700394.

10. Nopparat J, Nualla-Ong A, Phongdara A. Ethanolic extracts of Pluchea indica (L.) leaf pretreatment attenuates cytokine-induced β-cell apoptosis in multiple low-dose streptozotocin-induced diabetic mice. PLoS One. 2019;14(2):e0212133. DOI: 10.1371/journal.pone.0212133; PMID: 30779805; PMCID: PMC6380574.

11. Nopparat J, Nualla-Ong A, Phongdara A. Treatment with Pluchea indica (L.) Less. leaf ethanol extract alleviates liver injury in multiple low-dose streptozotocin-induced diabetic BALB/c mice. Exp Ther Med. 2020;20(2):1385-96. DOI: 10.3892/etm.2020.8877; PMID: 32742373; PMCID: PMC7388285.

12. Franco C, Sciatti E, Favero G, Bonomini F, Vizzardi E, Rezzani R. Essential Hypertension and Oxidative Stress: Novel Future Perspectives. Int J Mol Sci. 2022;23(22):14489. DOI: 10.3390/ijms232214489; PMID: 36430967; PMCID: PMC9692622.

13. Valentini A, Heilmann RM, Kühne A, Biagini L, De Bellis D, Rossi G. The Renin-Angiotensin-Aldosterone System (RAAS): Beyond Cardiovascular Regulation. Vet Sci. 2025;12(8):777. DOI: 10.3390/vetsci12080777; PMID: 40872727; PMCID: PMC12390185.

14. Griendling KK, Camargo LL, Rios FJ, Alves-Lopes R, Montezano AC, Touyz RM. Oxidative Stress and Hypertension. Circ Res. 2021;128(7):993-1020. DOI: 10.1161/CIRCRESAHA.121.318063; PMID: 33793335; PMCID: PMC8293920.

15. Daneshzad E, Keshavarz SA, Qorbani M, Larijani B, Azadbakht L. Dietary total antioxidant capacity and its association with sleep, stress, anxiety, and depression score: A cross-sectional study among diabetic women. Clin Nutr ESPEN. 2020;37:187-94. DOI: 10.1016/j.clnesp.2020.03.002; PMID: 32359742.

16. Manoharan S. Is It Still Relevant to Discover New ACE Inhibitors from Natural Products? YES, but Only with Comprehensive Approaches to Address the Patients' Real Problems: Chronic Dry Cough and Angioedema. Molecules. 2023;28(11):4532. DOI: 10.3390/molecules28114532. PMID: 37299008; PMCID: PMC10254462.

17. Akif M, Georgiadis D, Mahajan A, Dive V, Sturrock ED, Isaac RE, et al. High-resolution crystal structures of Drosophila melanogaster angiotensin-converting enzyme in complex with novel inhibitors and antihypertensive drugs. J Mol Biol. 2010;400(3):502-17. DOI: 10.1016/j.jmb.2010.05.024; PMID: 20488190.

18. Humphrey W, Dalke A, Schulten K. VMD: visual molecular dynamics. J Mol Graph. 1996;14(1):33-8. DOI: 10.1016/0263-7855(96)00018-5. PMID: 8744570.

19. Tian W, Chen C, Lei X, Zhao J, Liang J. CASTp 3.0: computed atlas of surface topography of proteins. Nucleic Acids Res. 2018;46(W1):W363-W367. DOI: 10.1093/nar/gky473; PMID: 29860391; PMCID: PMC6031066.

20. Myung Y, de Sá AGC, Ascher DB. Deep-PK: deep learning for small molecule pharmacokinetic and toxicity prediction. Nucleic Acids Res. 2024;52(W1):W469-75. DOI: 10.1093/nar/gkae254; PMID: 38634808; PMCID: PMC11223837.

21. Eberhardt J, Santos-Martins D, Tillack AF, Forli S. AutoDock Vina 1.2.0: New Docking Methods, Expanded Force Field, and Python Bindings. J Chem Inf Model. 2021;61(8):3891-8. DOI: 10.1021/acs.jcim.1c00203; PMID: 34278794; PMCID: PMC10683950.

22. Masuyer G, Schwager SL, Sturrock ED, Isaac RE, Acharya KR. Molecular recognition and regulation of human angiotensin-I converting enzyme (ACE) activity by natural inhibitory peptides. Sci Rep. 2012;2:717. DOI: 10.1038/srep00717; PMID: 23056909; PMCID: PMC3466449.

23. Zheng W, Tian E, Liu Z, Zhou C, Yang P, Tian K, et al. Small molecule angiotensin converting enzyme inhibitors: A medicinal chemistry perspective. Front Pharmacol. 2022;13:968104. DOI: 10.3389/fphar.2022.968104; PMID: 36386190; PMCID: PMC9664202.

24. Pratama MRF, Poerwono H, Siswodiharjo S. ADMET properties of novel 5-O-benzoylpinostrobin derivatives. J Basic Clin Physiol Pharmacol. 2019;30(6):20190251. DOI: 10.1515/jbcpp-2019-0251; PMID: 31851612.

25. Yu F, Zhang Z, Luo L, Zhu J, Huang F, Yang Z, et al. Identification and Molecular Docking Study of a Novel Angiotensin-I Converting Enzyme Inhibitory Peptide Derived from Enzymatic Hydrolysates of *Cyclina sinensis*. Mar Drugs. 2018;16(11):411. DOI: 10.3390/md16110411; PMID: 30373231; PMCID: PMC6265983.

26. Thompson MW. Regulation of zinc-dependent enzymes by metal carrier proteins. Biometals. 2022;35(2):187-213. DOI: 10.1007/s10534-022-00373-w; PMID: 35192096; PMCID: PMC8862405.

27. Rowland R, Brandariz-Nuñez A. Analysis of the Role of N-Linked Glycosylation in Cell Surface Expression, Function, and Binding Properties of SARS-CoV-2 Receptor ACE2. Microbiol Spectr. 2021;9(2):e0119921. DOI: 10.1128/Spectrum.01199-21; PMID: 34494876; PMCID: PMC8557876.

28. El-Baba TJ, Lutomski CA, Burnap SA, Bolla JR, Baker LA, Baldwin AJ, et al. Uncovering the Role of N-Glycan Occupancy on the Cooperative Assembly of Spike and Angiotensin Converting Enzyme 2 Complexes: Insights from Glycoengineering and Native Mass Spectrometry. J Am Chem Soc. 2023;145(14):8021-32. DOI: 10.1021/jacs.3c00291; PMID: 37000485; PMCID: PMC10103161.

29. El-Feky AM, El-Rashedy AA, Ibrahim NE. Computational and bioactivity investigations of flavonoid fraction from Dodonaea viscosa against oxidative stress and inflammation. Sci Rep. 2025;15(1):43652. DOI: 10.1038/s41598-025-29576-0; PMID: 41381691; PMCID: PMC12701060.

30. Zhuo C, Zeng C, Liu H, Wang H, Peng Y, Zhao Y. Advances and Mechanisms of RNA-Ligand Interaction Predictions. Life. 2025;15(1):104. DOI: 10.3390/life15010104; PMID: 39860045; PMCID: PMC11767038.

31. Loeffler JR, Fernández-Quintero ML, Schauperl M, Liedl KR. STACKED - Solvation Theory of Aromatic Complexes as Key for Estimating Drug Binding. J Chem Inf Model. 2020;60(4):2304-13. DOI: 10.1021/acs.jcim.9b01165; PMID: 32142283; PMCID: PMC7189365.

32. Carlsson AC, Scholfield MR, Rowe RK, Ford MC, Alexander AT, Mehl RA, et al. Increasing Enzyme Stability and Activity through Hydrogen Bond-Enhanced Halogen Bonds. Biochemistry. 2018;57(28):4135-47. DOI: 10.1021/acs.biochem.8b00603; PMID: 29921126; PMCID: PMC6052408.